Int. J. Heat Mass Transfer. Vol. 28, No. 1, pp. 69–80, 1985
Printed in Great Britain

0017–9310/85 $3.00 + 0.00

The influence of liquid viscosity and system pressure on stagnation point vapour thickness during forced-convection film boiling

T. R. FODEMSKI*
Warsaw Technical University

(*Received* 1 *August* 1983; *in revised form* 30 *April* 1984)

Abstract—The theoretical model of forced-convection film boiling in the stagnation point region of an axisymmetrical particle is demonstrated. Due to the 'lubrication effect' of the laminar vapour flow around the hot particle the liquid flow is slightly perturbed from the frictionless flow. This perturbation depends upon particle surface, free-stream and saturation temperatures. The effect of vapour velocity from the interface, towards the hot surface, on the heat flux conducted from the particle is taken into account. An attempt has been made to include the influence of the system pressure on the phenomenon—so the presented model can be utilized in the description of the coarse premixing phase during vapour (thermal) explosion. The applicability of the model to the calculation of vapour layer thickness in the stagnation point of the sphere and also of heat fluxes at the interface and at the hot surface (the important parameters which influence stability and film boiling collapse) is shown.

1. INTRODUCTION

FORCED-convection film boiling results from the relative motion between a hot particle and a cool liquid. This is believed to be an important mode of heat transfer during vapour explosions, both during the coarse premixing phase and during later stages (when the system pressure beings to decay and vapour may be present).

The calculation of vapour layer thickness at the stagnation point is of considerable importance to vapour explosion theory. The vapour thickness, minimal at the stagnation point, determines not only the heat flux from the hot particle, but also influences the stability [1] and collapse of the film boiling, which can be self-triggered or caused by a pressure pulse (shock wave). This vapour collapse is particularly important, since it may lead to a violent vapour (thermal) explosion.

The theoretical analysis presented here is seen as an improvement on those given by the authors of [2, 3] despite the fact that it is strictly limited to the stagnation point. With comparison to the works [2] and [3] assumptions regarding flow and heat transfer in the vapour are more realistic, and unlike in [3] the viscosity of the liquid (and deviation from frictionless flow) is taken into account. An attempt has also been made to include the influence of the system pressure on this phenomenon. As an example of application the results of calculation for water [10] are presented.

2. PHYSICAL MODEL

The main aims of the work are:

—detailed analysis of the heat transfer in the vapour,
—to take account of liquid viscosity, i.e. distortion of the liquid flow from the frictionless case.

These will be included in the model described, which leads to the calculation of the vapour layer thickness and of the heat flux in the neighbourhood of the stagnation point of an axisymmetrical particle. A curvilinear system of coordinates is chosen (see Fig. 1), where x is the length measured along any meridian from the front stagnation point and y is the coordinate normal to the surface of the particle.

The following assumptions have been made:

1. The vapour layer is very thin compared with the sphere radius ($\delta \ll R$).
2. The vapour velocity has two components: one in the x direction and one in the y. The laminar flow of vapour around the particle occurs as a result of the motion of the liquid at the interface and also because of a pressure gradient produced by the liquid flow (pressure gradient in the vapour film is taken to be the same). The vapour velocity towards the hot surface varies from a maximum at the interface to zero at the hot surface.
3. Due to liquid viscosity the liquid flow in the stagnation point region is slightly perturbed from the frictionless flow.
4. The temperature at the liquid–vapour interface is constant at the saturation value T_s. The free-stream liquid temperature T_∞ and velocity U_∞, the surface

---

* Present address: Simon Engineering Laboratories, Nuclear Department, University of Manchester, M13 9PL, England.

NOMENCLATURE

a	constant, defined by equation (A26)
A	constant, stagnation point velocity gradient
b	constant, defined by equation (A27)
B	constant, coefficient in heat balance equation
c_p	specific heat at constant pressure
C	constant, defined by equation (24)
F	dimensionless fluid flow stream function
$g(y_*)$	function defined by equation (48)
$G(\lambda_*)$	function defined by equation (47)
h	latent heat
k	thermal conductivity
l	dimensionless perturbation function
m	evaporation mass rate
M	mass flow rate
p	pressure
Pr	Prandtl number
q	heat flux
R	radius of sphere
T	temperature
ΔT	$= T_w - T_s$
ΔT_{subc}	$= T_s - T_\infty$
U	liquid velocity
W	fluid velocity
V	vapour velocity
x, y	coordinates
z	defined by equations (25) or (26).

Greek symbols

ε	emissivity
δ	vapour thickness
ζ	dimensionless similarity coordinate in fluid
θ	angle (in x direction)
μ	dynamic viscosity
ν	kinematic viscosity
κ	thermal diffusivity
λ	dimensionless vapour thickness
ρ	density
ξ	dummy variable
σ	radiant constant.

Subscripts

c	conduction
cnv	convection
ev	evaporation
l	value for liquid
o	no-shear stress value
r	radiation
s	saturation value
v	value for vapour
w	hot surface value
x	around the particle component
y	normal to the particle (or interface) component
∞	value at infinity (free stream)
*	normalised value.

Superscripts

—	mean value across vapour
f	value for a frictionless flow
h	hydrodynamic layer
o	value for vapour velocity $V_y = 0$
δ	value at the interface.

temperature $T_w > T_s$ of the particle are all constant and uniform.

5. All physical properties of the liquid and vapour are assumed to be constant and taken for average temperature (i.e. $(T_w + T_s)/2$ for the vapour and $(T_s + T_\infty)/2$ for the liquid).
6. Radiation heat transfer is included.

3. MOMENTUM EQUATION AND VELOCITY FIELD

The momentum equation for a fluid in the region of the stagnation point has the general form [4, 5]:

$$F''' + \alpha F F'' + \beta(1 - F'^2) = 0, \tag{1}$$

where F-dimensionless fluid flow stream function, with boundary conditions, in this case specified in the form

$$F(0) = F_o, \quad F'(0) = F_1, \quad F'(\zeta = H) = F_2, \tag{2}$$

where ζ is the dimensionless similarity coordinate.

The values of α and β depend upon the shape of the body; the constants F_o, F_1, F_2 and H depend upon the nature of the problem.

For an axisymmetrical particle the values of α and β are 1 and $\frac{1}{2}$ respectively, and a well known solution of equation (1), and velocity components for the frictionless fluid are then [5]:

$$F(\zeta) = \zeta = \sqrt{\frac{2A}{\nu}}\, y, \tag{3}$$

$$W_x = Ax \frac{\mathrm{d}F}{\mathrm{d}\zeta} = Ax, \tag{4}$$

$$W_y = -\sqrt{2A\nu}\,F(\zeta) = -2Ay, \tag{5}$$

where A is the stagnation point velocity gradient (constant), and ν is the fluid kinematic viscosity. Note, that from equation (4), the normal gradient of x-compoment velocity is:

$$\frac{\partial W_x}{\partial y} = 0. \tag{6}$$

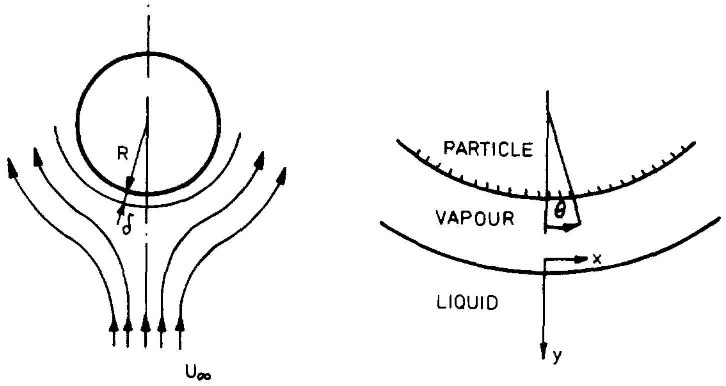

FIG. 1. Physical model and coordinate system.

For a viscous liquid, when the temperature T_w of the surface of the particle is less than T_s, the liquid velocity components at $y = 0$ are zero and, as a result of this, the liquid flow departs from the frictionless solution for a thin layer. For the case discussed ($T_w > T_s$) however, the particle is covered by vapour (acting as a 'lubricator') and the liquid flow departure, from the frictionless case is less dramatic than for the $T_w < T_s$ case. In the 'lubricator' case the vapour flow influences the liquid flow. The latter, however, can be exactly as given by equations (3) to (6) provided that the boundary condition F_0 and F_1—now taken at the liquid–vapour interface—are appropriate.

Equation (1) will be discussed for the liquid case in Section 3.1 and for the vapour case in Section 3.2, followed by a discussion, in Section 3.3, of the appropriate matching conditions at the liquid–vapour interface.

3.1 *Liquid flow*

Solution of equation (1) assuming slight perturbation of the liquid flow from frictionless case [5] is given in Appendix 1. Utilizing this solution, the liquid velocity components and the pressure gradient at the interface can be expressed as

$$U_x(0) = A_l x(1+u_*), \tag{7}$$

$$U_y(0) = -\sqrt{2A_l\nu_l}\,l(0) \cong 0, \tag{8}$$

$$\left(-\frac{\partial p}{\partial x}\right)_{l,y=0} = \rho_l A_l^2 \times (1+u_*^2). \tag{9}$$

Coefficient u_*, which expresses the deviation of liquid interface velocity, $U_x(0)$, from the velocity $U_x^f(0)$ for the frictionless flow case, is:

$$u_* = l'(0) = F_1'(0) - 1 = \frac{U_x(0) - U_x^f(0)}{U_x^f(0)}. \tag{10}$$

3.2 *Vapour flow*

According to Assumption 2 we can write:

$$\left(-\frac{\partial p}{\partial x}\right)_v = \rho_v A_v^2 x = \left(-\frac{\partial p}{\partial x}\right)_{l,y=0} = \rho_l A_l^2 x(1+u_*^2) \tag{11}$$

and

$$A_v = A_l\sqrt{\rho_*(1+u_*^2)}, \tag{12}$$

where

$$\rho_* = \rho_l/\rho_v. \tag{13}$$

Solution of equation (1) for vapour—neglecting the effect of inertia (vapour flow in the thin layer is governed by viscous and pressure forces)—is given in Appendix 2. Utilizing this solution and introducing the following dimensionless parameters:

$$y_* = \frac{y}{\delta} = \frac{\zeta_v}{\zeta_v^\delta}, \quad \lambda_* = \frac{\lambda}{\lambda_o}, \quad \lambda_o = \sqrt{\frac{Pr_v}{\rho_*}}, \tag{14}$$

where

$$\zeta_v^\delta = \zeta_v(\delta) = \sqrt{\frac{2A_v}{\nu_v}}\,\delta = 2\lambda_*\left(\frac{1+u_*^2}{\rho_*}\right)^{1/4},$$

$$\lambda = \delta\sqrt{\frac{A_l}{2\kappa_v}}, \tag{15}$$

the vapour velocity components, V_x and V_y, the mean vapour velocity, $\bar{V}_x$, and vapour mass flow, M_v, in the vapour gap of thickness δ, can be expressed as follows:

$$V_x = A_v x(C - \tfrac{1}{4}\zeta_v^\delta y_*)\zeta_v^\delta y_*, \tag{16}$$

$$V_y = -\sqrt{\tfrac{1}{2}A_v\nu_v}\,(C - \tfrac{1}{6}\zeta_v^\delta y_*)\zeta_v^{\delta 2} y_*^2, \tag{17}$$

$$\bar{V}_x = \int_0^1 V_x(y_*)\,\mathrm{d}y_* = \tfrac{1}{2}A_v\zeta_v^\delta x(C - \tfrac{1}{6}\zeta_v^\delta), \tag{18}$$

$$M_v = \bar{V}_x\rho_v 2\pi x\cdot\delta(x). \tag{19}$$

The integration constant C will be determined from the interface matching conditions.

The mass flow M_v, equation (19) can be related to the local evaporation rate, m, from the interface, i.e.

$$m = \frac{\mathrm{d}M_v}{2\pi x\,\mathrm{d}x} = \rho_v\left[\left(\frac{\mathrm{d}\bar{V}_x}{\mathrm{d}x} + \frac{\bar{V}_x}{x}\right)\delta + \bar{V}_x\frac{\mathrm{d}\delta}{\mathrm{d}x}\right] = \rho_v V_y(\delta). \tag{20}$$

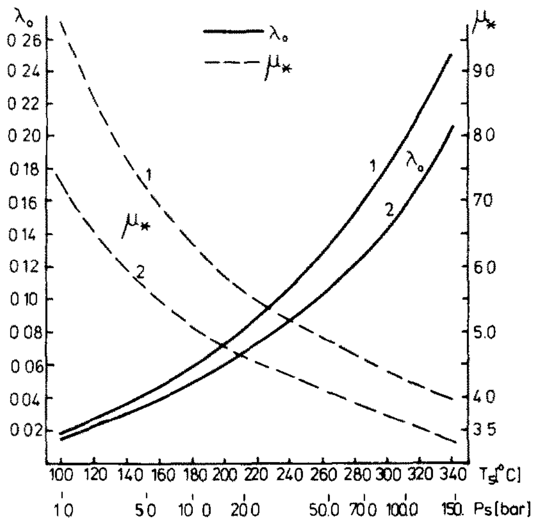

FIG. 2. Pressure influence on dimensionless values of λ_0 and μ_*, 1—$\Delta T = 500$°C, $\Delta T_{\text{subc}} = 40$°C; 2—$\Delta T = 1000$°C, $\Delta T_{\text{subc}} = 0$°C.

3.3 *Matching conditions*

Matching conditions at the liquid–vapour interface are:

$$U_x(0) = V_x(\delta), \tag{21}$$

$$\mu_1 \left.\frac{\partial U_x}{\partial y}\right|_0 = \mu_v \left.\frac{\partial V_x}{\partial y}\right|_\delta, \tag{22}$$

$$\rho_1 U_y(0) = \rho_v V_y(\delta). \tag{23}$$

Using the first matching condition, the constant C can be expressed by equation:

$$C = \frac{1+u_* + \lambda_*^2(1+u_*^2)}{2\lambda_*(1+u_*^2)^{3/4}\cdot\rho_*^{1/4}}. \tag{24}$$

Now equation (20) can be written in the form:

$$(\lambda_0\lambda_*)^2[1+u_* + \tfrac{1}{3}\lambda_*(1+u_*^2)]\left(1 + \frac{x}{2\lambda_*}\frac{\mathrm{d}\lambda_*}{\mathrm{d}x}\right) = z^2 \tag{25}$$

and

$$z^2 = \delta \cdot V_y(\delta)/2\kappa_v. \tag{26}$$

At the stagnation point we have $\mathrm{d}\lambda_*/\mathrm{d}x = 0$.

The second matching condition, using equations (A1), (A3), (A16), (7), (16) and (24) can be written in the form:

$$-\lambda_*\mu_* u_* = (1+u_*)\left(1 - \lambda_*^2 \frac{1+u_*^2}{1+u_*}\right), \tag{27}$$

where

$$\mu_* = \sqrt{2\pi\mu_1/\mu_v}. \tag{28}$$

From equation (27) it is clear that, for a given μ_* (equation (28), Fig. 2), we have (see Figs. 3 and 4):

(a) $u_* = 0$ when $\lambda_* = 1$. This means that there are no shear stresses at the liquid–vapour interface when the dimensionless vapour thickness $\lambda = \lambda_0$. The liquid flow is then identical to the frictionless flow (equations (3) to (6)). Note that the value of λ_0 (equation 14, Fig. 2) is independent of U_∞ and R, and is a function of fluid properties only.

(b) $u_* < 0$ when $\lambda_* < 1$, i.e. vapour is accelerated by liquid flow. This means that part of the kinetic energy of the liquid is both converted into kinetic energy of vapour and dissipated in the liquid viscous layer.

(c) $u_* > 0$ when $\lambda_* > 1$, i.e. liquid is accelerated by vapour flow. In this case a part of the heat flux from the hot particle causes an increase of the kinetic energy of the liquid (when compared with frictionless flow) and also dissipates in the liquid viscous layer. For $u_* > 0$ the final effect of the liquid viscosity is that it slightly improves the heat transfer from the hot particle (see Discussion and Fig. 7).

The distortion u_* of the liquid velocity from frictionless flow takes place only in the boundary layer. The dimensionless thickness of this layer, ζ_1^{h}, can be calculated from equation (A7) using the criterion, common in boundary layer theory, that inside the layer, the distortion from the frictionless flow is greater than 1% [4, 5]. This leads to the relation (see Fig. 5)

$$u_*\left[\exp(-\tfrac{1}{2}\zeta_1^{\text{h}2}) - \sqrt{\frac{\pi}{2}}\,\zeta_1^{\text{h}}\,\mathrm{erfc}\left(\frac{1}{\sqrt{2}}\zeta_1^{\text{h}}\right)\right] = 0.01. \tag{29}$$

Clearly, a direct relation $\zeta_1^{\text{h}} = f(\lambda_*)$ based on equations (27) and (29) exists.

The present analysis has been limited to the case of the stagnation region. Nevertheless, it is clear that the

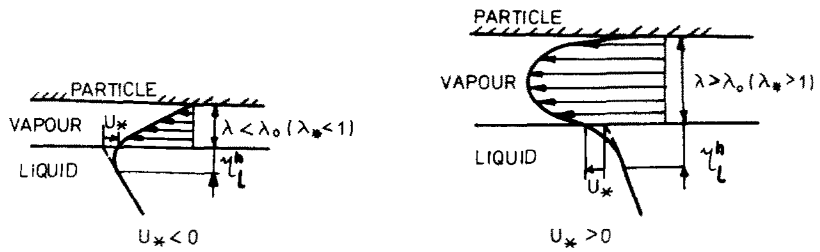

FIG. 3. Vapour and liquid velocity distributions and vapour thickness influence on interface velocity.

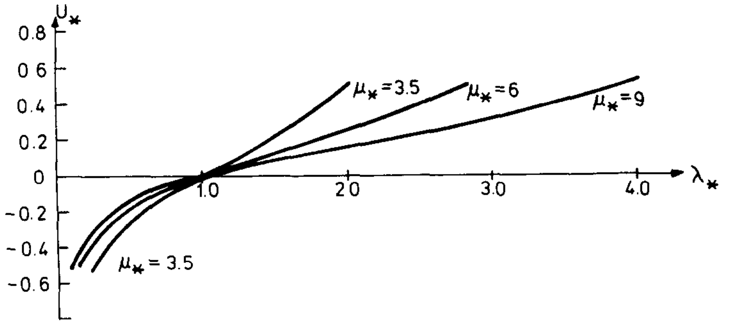

FIG. 4. The influence of the dimensionless, normalized thickness, λ_*, on the coefficient u_* (distortion of the interface velocity from a frictionless case).

distortion of the liquid flow changes when moving away from this region towards the equatorial plane of the particle. This is because at the interface the pressure gradient and the velocity are functions of θ (see Fig. 1). An account of that, for a different case, i.e. motion of a spherical gas bubble in a viscous liquid is discussed in refs. [6] and [7]. However, the assumptions and simplifications made in both works are such that the momentum equation and the flow solution are not valid for the front stagnation point region—where equation (1) with boundary conditions, and distortion from the frictionless solution, given by equations (2) and (3) should be considered. This fact is clearly stated by the authors of both works (see, particularly, discussion in [6]).

Moreover, there is another reason for distinguishing the present analysis from that given in [6] and [7]: here, apart from the effect of the pressure gradient and velocity at the interface, the distortion of the liquid flow is a function of vapour velocity profile, i.e. vapour layer thickness. The value of the latter around the particle strongly depends upon its value at the stagnation point. Its accurate calculation at the stagnation point is therefore paramount. For the moving bubble, the vapour flow is different: the vapour circulates inside the bubble. In [6] the allowance is made for interface interaction between vapour and liquid flows. In [7] this effect is neglected and the latter differs from potential flow only as a result of vanishing liquid tangential stresses at the bubble surface.

The results of the stagnation point analysis presented here are, however, consistent with [6] and [7]. When the liquid accelerates the vapour flow—this is always the case discussed in [6]—both the presented analysis and that of [6] predict $u_* < 0$. Neglecting vapour flow interaction, as in [7], the tangential stresses in the liquid at the interface should be zero. They are, but only exactly so, for the stagnation point frictionless solution (see equation (6)) and therefore, according to [7], the liquid flow is undisturbed at that point. If, however, vapour flow is taken into account this can only happen for particular value of $\lambda = \lambda_0$. For the reasons explained the present analysis, although limited to the stagnation point, should be regarded as more general than the analyses of [6] and [7].

4. HEAT TRANSFER

The energy equation for a fluid in the region of the stagnation point has the general form [4, 5]:

$$t'' + \alpha \cdot PrF(\zeta)t' = 0 \qquad (30)$$

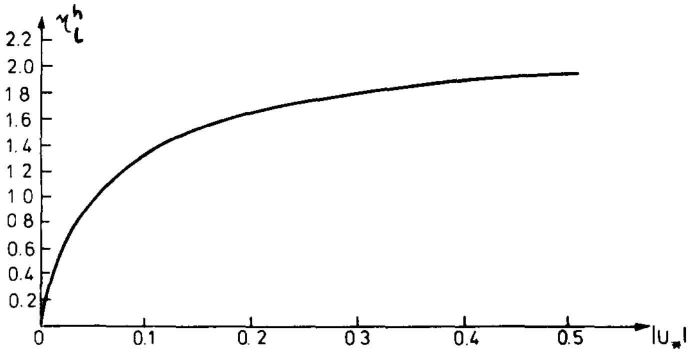

FIG. 5. Dimensionless hydrodynamic layer thickness, ζ_l^h, as a function of the interface velocity distortion (from a frictionless case), u_*.

where $t(\zeta)$ is the dimensionless fluid temperature, with boundary conditions in this case specified in the form

$$t(0) = 0, \quad t(H) = 1. \tag{31}$$

For an axisymmetrical particle the value of α is 1 and the solution of equation (30) is of the form

$$t'(\zeta) = e(\zeta)/E(H), \tag{32}$$

and

$$t(\zeta) = E(\zeta)/E(H),$$

where

$$e(\zeta) = \exp\left[-Pr\int_0^{\zeta} F(\xi)\,d\xi\right], \tag{33}$$

$$E(\zeta) = \int_0^{\zeta} e(\xi)\,d\xi, \tag{34}$$

and ξ is a dummy variable.

4.1 *In the liquid*

The dimensionless liquid temperature is expressed by the equation

$$t_l(\zeta_l) = \frac{T(\zeta_l) - T_s}{T_\infty - T_s}. \tag{35}$$

Using equation (32) the heat flux convected into the liquid can be expressed as follows:

$$q_{cnv} = -k_l \left.\frac{dT_l}{dy}\right|_{y=0} = k_l \left.\frac{dt_l}{d\zeta_l}\right|_0 \frac{d\zeta_l}{dy}(T_s - T_\infty)$$

$$= E_l^{-1}(\infty)\sqrt{\frac{2A_l}{\nu_l}}\,k_l(T_s - T_\infty) \tag{36}$$

where

$$E_l(\infty) = \int_0^{\infty} \exp\left[-Pr_l \int_0^{\zeta_l} F_l(\xi)\,d\xi\right] d\zeta_l, \tag{37}$$

and

$$F_l(\zeta_l) = \zeta_l + l(\zeta_l).$$

The analytical expressions for the function $l(\zeta_l)$ and its integral are given by equations (A9) and (A10), see Appendix 1.

The coefficient $E_l(\infty)$ and the heat flux convected into the liquid for the frictionless case, i.e. when $F_l(\zeta_l) = \zeta_l$, are expressed by the equations

$$E_l^f(\infty) = \int_0^{\infty} \exp\left[-\tfrac{1}{2}Pr_l\zeta_l^2\right] d\zeta_l$$

$$= \sqrt{\frac{\pi}{2Pr_l}}\,\mathrm{erf}(\infty) = \sqrt{\frac{\pi}{2Pr_l}}, \tag{38}$$

and

$$q_{cnv}^f = 2k_l\sqrt{\frac{Pr_l A_l}{\pi\nu_l}}\,(T_s - T_\infty). \tag{39}$$

For the spherical particle the value of A_l is $3U_\infty/2R$ and then

$$q_{cnv}^f = k_l\sqrt{\frac{6U_\infty}{\pi R\kappa_v}}\,(T_s - T_\infty). \tag{40}$$

This result is identical to that given by Chao [8] where the fluid sphere is moving through another fluid of large extent and it is assumed that the flow field in the latter is a potential one. The heat flux given by equation (40) was used in analyses [2] and [3], i.e. the influence of the distortion of the liquid flow from the frictionless case on heat transfer in the liquid was neglected. The measure of this effect is the ratio of the two fluxes discussed, i.e.

$$K(u_*) = \frac{q_{cnv}}{q_{cnv}^f} = \sqrt{\frac{\pi}{2Pr_l}}\,E_l^{-1}(\infty). \tag{41}$$

The integral $E_l(\infty)$ expressed by equation (37), when $l(\zeta_l) \neq 0$, must be calculated numerically.

4.2 *In the vapour*

The dimensionless vapour temperature is expressed by the equation

$$t_v(\zeta_v) = \frac{T_v(\zeta) - T_w}{T_s - T_w}. \tag{42}$$

Using equation (32) the heat fluxes at the hot surface ($y = 0$) and at the interface ($y = \delta$), due to conduction through the vapour, are

$$q_w = q(0) = -k_v\left.\frac{dT_v}{dy}\right|_0 = k_v t_v'(0)\frac{d\zeta_v}{dy}(T_w - T_s)$$

$$= E_v^{-1}(\zeta_v^\delta)\sqrt{\frac{2A_v}{\nu_v}}\,k_v(T_w - T_s) \tag{43}$$

$$q_c^\delta = q(\delta) = -k_v\left.\frac{dT_v}{dy}\right|_\delta = k_v t_v'(\zeta_v^\delta)\frac{d\zeta_v}{dy}$$

$$\times (T_w - T_s) = q_w e_v(\zeta_v^\delta). \tag{44}$$

The integrals across the vapour, $e_v(\zeta_v^\delta)$ and $E_v(\zeta_v^\delta)$ (see equations (33) and (34)), can be expressed in terms of y_*, λ_* and λ_0 (see Appendix 3).

Using this transformation the heat fluxes considered can be written in the form

$$q_w = k_v\frac{T_w - T_s}{\delta}\,G(\lambda_*)\exp\left[g(\lambda_*, 1)\right], \tag{45}$$

$$q_c^\delta = k_v\frac{T_w - T_s}{\delta}\,G(\lambda_*), \tag{46}$$

where

$$G(\lambda_*) = \left\{\exp\left[g(\lambda_*, 1)\right]\int_0^1 \exp\left[-g(\lambda_*, y_*)\right] dy_*\right\}^{-1}, \tag{47}$$

$$g(\lambda_*, y_*) = a(\lambda_*)y_*^3\left[1 - b(\lambda_*)y_*\right]. \tag{48}$$

The coefficients $a(\lambda_*)$ and $b(\lambda_*)$ are expressed by equations (A26) and (A27), see Appendix 3.

Because of the movement of the vapour towards the particle, with velocity $V_y(y)$, the heat fluxes expressed by equations (45) and (46) are not equal. When this effect is neglected, i.e. $V_y(y) = 0$, then the temperature distribution in the vapour gap is linear and these fluxes are the same and equal:

$$q_c^o = k_v \frac{T_w - T_s}{\delta}. \qquad (49)$$

The measure of this effect is the ratio of two heat fluxes, expressed by equations (46) and (49) respectively, i.e. coefficient given by equations (47), which must be calculated numerically.

4.3 *At the liquid–vapour interface*

A part (q_{cnv}) of the heat flux ($q_c^\delta + q_r$), transferred from the hot particle through the vapour layer, is convected into the liquid at the interface; the remainder (q_{ev}) produces a vapour mass flow, m, towards the sphere. Thus equation governing the heat balance at the interface can be written as

$$q_c^\delta + q_r = q_{cnv} + q_{ev}, \qquad (50)$$

where

$$q_{ev} = m \cdot h, \qquad (51)$$

$$q_r = \sigma(\varepsilon_w^{-1} + \varepsilon_l^{-1} - 1)(T_w^4 - T_s^4), \qquad (52)$$

and h is the latent heat, ε is the emissivity, σ is the radiant constant.

Using equations (20), (26), (36), (44) and (52) the heat balance equation can be written in the form:

$$B_c \cdot G(\lambda_*) + \{B_r - B_{cnv} \cdot K[u_*(\lambda_*)]\} \cdot \lambda_* = z^2 \qquad (53)$$

where

$$B_c = \frac{\Delta T \cdot c_p v}{2h} \qquad (54)$$

$$B_{cnv} = \frac{2 \cdot \Delta T_{subc} \cdot c_{pv} \cdot k_l}{\sqrt{Pr_l} \cdot h \cdot \mu_* \cdot k_v} \qquad (55)$$

and

$$B_r = \frac{\sigma \cdot (T_w^4 - T_s^4) \cdot (\varepsilon_w^{-1} + \varepsilon_l^{-1} - 1) \cdot \lambda_o}{\rho_v h \cdot \sqrt{2\kappa_v A_l}}. \qquad (56)$$

Using equations (53), (26), (27), (41) and (47) we can calculate λ_* for given values of ΔT and ΔT_{subc}. Only the coefficient B_r expressed by equation (56) depends upon the stagnation point velocity gradient A_l in the liquid. Therefore, if the heat flux due to radiation can be neglected, the dimensionless vapour thickness λ_* calculated from equation (53) depends upon the temperatures T_w, T_s and T_∞ only, is valid for all axisymmetrical particles and is independent of U_∞ (liquid velocity).

The vapour thickness δ for particular values of λ_* can be calculated using equation (15) and depends upon A_l.

5. RESULTS AND DISCUSSION

The foregoing theory has been used as the basis of a numerical calculation for the case of water—the most widely used coolant for nuclear reactors. Most such reactors are pressurized, so any analysis of fuel–coolant mixing should take account of this. Furthermore, the initial stage of a thermal explosion is characterized by a local self-pressurization. Since system pressure is the paramount influence on the vapour thickness surrounding a hot particle during forced convection film boiling the calculations have been carried out for a range of such pressures.

Figure 2 shows the influence of the system pressure (or saturation temperature) on λ_o and μ_* (see equations (14) and (28) respectively).

Figure 4 shows the relation $u_* = f(\lambda_*)$ for different values of μ_* (see equation (27)). It is clear that dimensionless normalized vapour thickness λ_* can substantially affect liquid velocity at the interface so this should be taken into account, particularly for system pressure greater than atmospheric, i.e. $\mu_* < 9$. In line with Assumption 3 all calculations have been carried out for $|u_*| < 0.5$.

Figure 6 shows the influence of the distortion of liquid flow (from the frictionless case) on the heat flux convected into the liquid. The latter is normalized as a fraction of q_{cnv}^f, and the measure of the above influence is given by the coefficient $K(u_*)$ as given by equation (41). The influence of system pressure and liquid temperature is shown by plotting separate curves for two different values, i.e. 0.8 and 5.0 of Prandtl number. For $u_* > 0$ the improvement in heat transfer in the liquid due to its viscosity is noticeable, for $u_* < 0$ the heat flux convected into the liquid decreases.

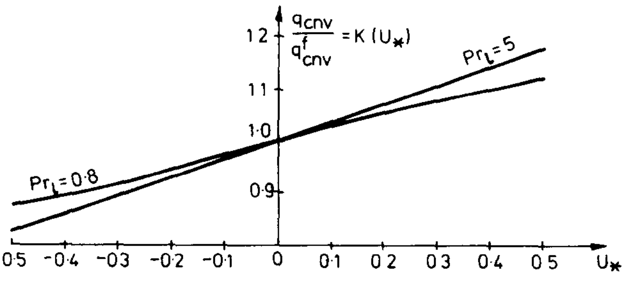

FIG. 6. The influence of the interface velocity distortion, u_*, on the heat flux convected into the liquid.

Figure 7 shows the influence, on the heat fluxes q_w and q_c^δ conducted from the hot particle, of

(i) the vapour velocity, $V_y(y)$, towards a sphere,
(ii) the liquid viscosity.

The first effect, although neglected in almost all previous analyses of film boiling heat transfer, can be significant: it grows in importance with the value of λ_o (i.e. with pressure—see Fig. 2). To show this more clearly the heat flux at the interface (q_c^δ of equation (44)) is presented as a function of λ_*. The heat flux is normalized as a fraction of q_c^o (expressed by equation (49)) where it is assumed that there is no vapour velocity towards the sphere, but the vapour thickness, δ, is the same. Figure 7 also shows the ratio of two heat fluxes q_w and q_c^δ as a function of λ_*. These ratios are expressed by functions $G(\lambda^*)$ and $\exp[g(\lambda^*)]$ respectively (see equations (45) to (48)). They differ in form from those of work [3], this being the result of more realistic and accurate assumptions regarding the liquid and vapour flows and the heat transfer in the vapour (discussed in Sections 3.1, 3.2 and 4.2).

The influence of liquid viscosity on all the heat fluxes discussed is shown by calculating all quantities twice, for $u_* \neq 0$ (using equation (21) and the appropriate μ_* value—for the particular system pressure) and for $u_* = 0$. The latter therefore represents calculation based on the simplified model from the work [3], where liquid viscosity is neglected and gives comparison of results with the analysis presented here.

It is clear that for $\lambda_* > 1$ and for higher pressures the ratio of two heat fluxes q_w and q_c^δ calculated with the inclusion of the effect of liquid viscosity (i.e. $u_* > 0$) is greater than that calculated when the effect of liquid viscosity is neglected (i.e. $u_* = 0$). The difference increases with λ_o and can be regarded as a measure of the improvement in heat transfer in the vapour gap due to liquid viscosity. The system pressure influence is shown by plotting separate curves for different values of λ_o.

Figures 8 and 9 show the results of more extensive calculations based on the heat balance (equation (53)), for system pressures of 1 and 10 bars, and 100 and 150 bars respectively: the lines of constant values of λ_* cover wide ranges of $\Delta T = T_w - T_s$ and $\Delta T_{\text{subc}} = T_s - T_\infty$. In these calculations it was assumed that the ratio U_∞/R is 100 s^{-1}, and the emissivities, ε_w of the hot surface and ε_l of the water–vapour interface, are 0.8 and 0.9 respectively.

On Fig. 10 the division of the heat flux transferred through the vapour into components q_{ev*} and q_{cnv*} (A), and q_{r*} and q_{c*}^δ (B), is shown as a function of λ_*. As was mentioned the ratio q_r/q_c^δ depends upon the value of the velocity gradient, i.e. U_∞/R. Figure 10B shows the division of this heat flux into parts q_r and q_c^δ for three different values, 100, 50 and 25 s^{-1}, of U_∞/R when the system pressures are 1 bar and 150 bars. The influence of the velocity gradient on the components q_{ev*} and q_{cnv} (Fig. 10A) is negligible, in all the cases calculated being always less than 2%.

The results of the analysis presented give values of the heat flux q_c^δ and the vapour thickness δ of about 25–30% difference when compared with experimental data for atmospheric pressure [2, 9]. This is due to the fact that all experiments give average values of this flux for the bottom half of the sphere, where the vapour thickness is greater than at the stagnation point. Assessment of this variation in the vapour thickness can be found in [1] and [2]. However, in these works somewhat symbolistic models of the vapour and liquid flows and heat transfer were adopted. The present work provides a basis for calculating the variation of vapour thickness around the bottom half of the sphere more precisely. This, however, was not the aim of the present paper.

Finally, using Fig. 9 we can easily calculate the vapour thickness and heat flux q_c^δ for given values of ΔT

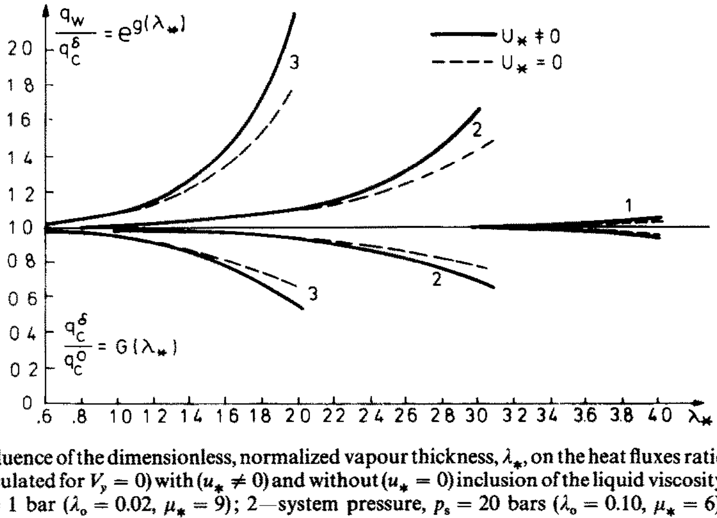

FIG. 7. The influence of the dimensionless, normalized vapour thickness, λ_*, on the heat fluxes ratios: q_w/q_c^δ and q_c^δ/q_c^o (q_c^o—calculated for $V_y = 0$) with ($u_* \neq 0$) and without ($u_* = 0$) inclusion of the liquid viscosity; 1—system pressure, $p_s = 1$ bar ($\lambda_o = 0.02$, $\mu_* = 9$); 2—system pressure, $p_s = 20$ bars ($\lambda_o = 0.10$, $\mu_* = 6$); 3—system pressure, $p_s = 150$ bars ($\lambda_o = 0.25$, $\mu_* = 3.5$).

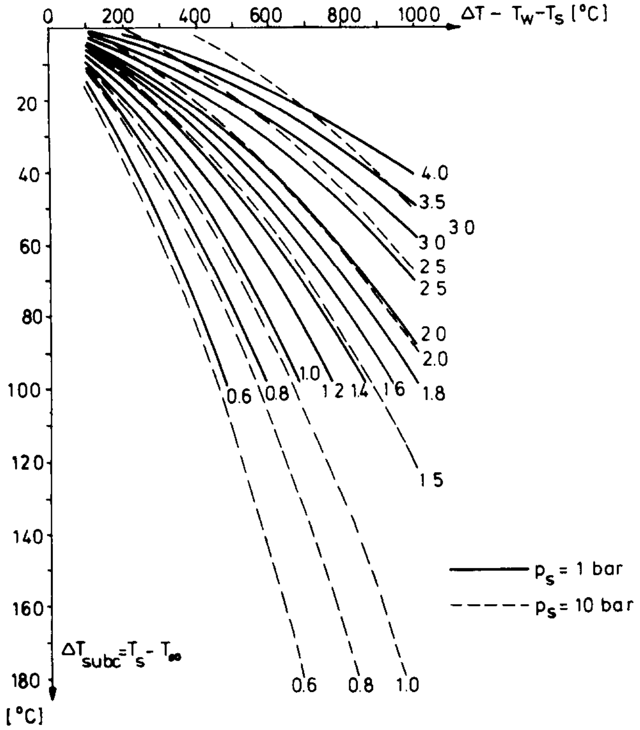

FIG. 8. Relation between $\Delta T = (T_w - T_s)$ and $\Delta T_{subc} = (T_s - T_\infty)$ for different values of dimensionless, normalized vapour thickness, λ_*.

and ΔT_{subc} when the pressure is 150 bars (although no experimental data are available). At $\Delta T = 1000°C$ and $\Delta T_{subc} \cong 45°C$, λ_* is approximately 2.1. At 150 bars and the mean vapour temperature $\bar{T}_v = 840°C$ the values of λ_0, κ_v, $\exp[g(\lambda_*)]$ and $G(\lambda_*)$ are 0.194, 1.65×10^{-6} m^2 s^{-1}, 1.83 and 0.86 respectively. We then found that, for example, at $R = 1$ cm and $U_\infty = 0.5$ m s^{-1} δ is 8.55 $\times 10^{-5}$ m, q_c^δ is 1.28 MW m^{-2}, q_r is 0.14 MW m^{-2} and q_{cmv} is 0.70 MW m^{-2}. The heat flux q_w at the hot surface is about 83% greater than q_c^δ.

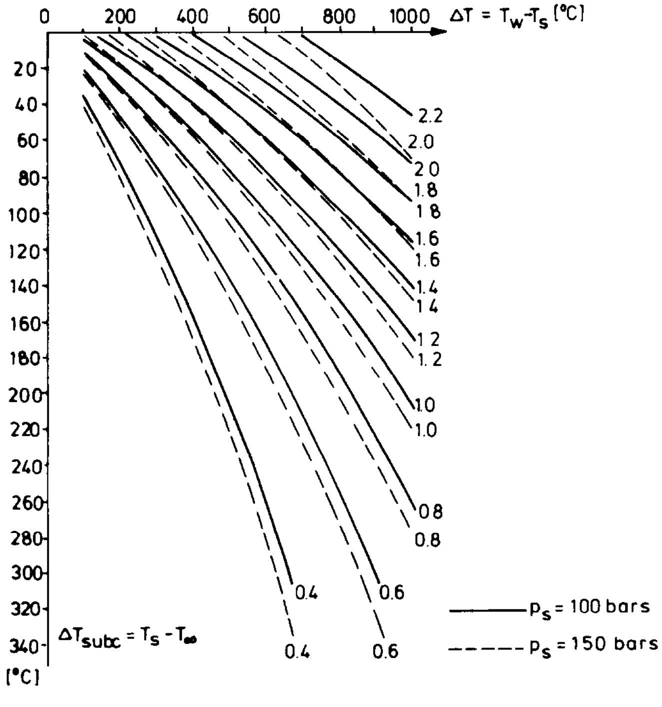

FIG. 9. Relation between $\Delta T = (T_w - T_s)$ and $\Delta T_{subc} = (T_s - T_\infty)$ for different values of dimensionless, normalized vapour thickness, λ_*.

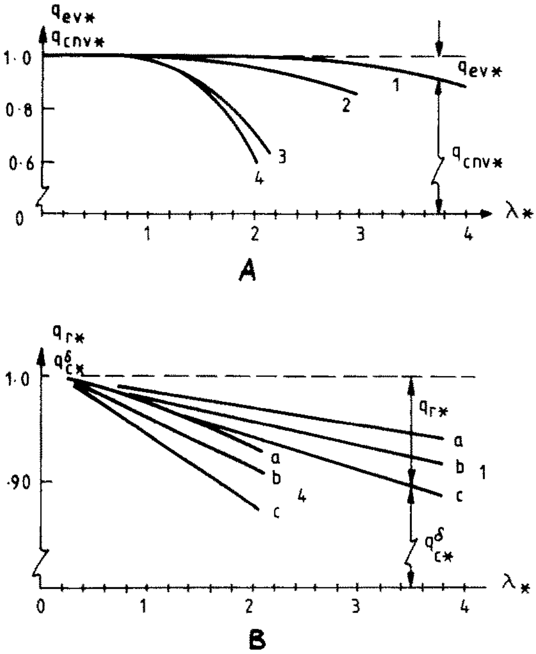

FIG. 10. The influence of the normalized vapour thickness λ_* on the division of the heat flux transferred from the hot particle $(q^{\delta}_c+q_r)$on two heat fluxes: (A) convected into liquid, $q_{cnv*} = q_{cnv}/(q^{\delta}_c+q_r)$, and causing evaporation from the interface, $q_{ev*} = mh/(q^{\delta}_c+q_r)$; (B) conducted through vapour, $q^{\delta}_{c*} = q^{\delta}_c/(q^{\delta}_c+q_r)$ and radiated from the hot surface, $q_{r*} = q_r/(q_c+q_r)$, for different U_{∞}/R: $100\,\mathrm{s}^{-1}$ (a), $50\,\mathrm{s}^{-1}$ (b) and $25\,\mathrm{s}^{-1}$ (c); 1—$p_s = 1$ bar; 2—$p_s = 10$ bars; 3—$p_s = 100$ bars; 4—$p_s = 150$ bars. In all cases $\Delta T = 1000$°C.

Calculating the same quantities using the simplified models, where the effects of liquid viscosity and velocity towards the hot sphere are neglected (i.e. $G(\lambda_*) = K(u_*) = 1$ in equation (53)), leads to the following values: δ is 1.05×10^{-4} m, the heat fluxes q_w and q^{δ}_c are the same and equal to $1.2\,\mathrm{MW\,m^{-2}}$, q_{cnv} is $0.61\,\mathrm{MW\,m^{-2}}$ and q_r is the same as previously. Thus the difference in the estimation of the vapour layer thickness δ is about $(-19)\%$, of the heat fluxes q_c, q_{cnv} and q_w 7%, 14% and 97% respectively. Inclusion of these more accurate estimates in the analyses of the stability, and of the collapse by a pressure pulse, of film boiling would substantially influence the result.

REFERENCES

1. T. R. Fodemski, Stagnation point oscillation and stability of forced convection film boiling on a sphere immersed in (a) subcooled or (b) superheated liquid, *Proc. 7th Int. Heat Transfer Conf. Munchen* **4**, 369–373 (1982).
2. M. Epstein and G. M. Hauser, Subcooled forced-convection film boiling in the forward stagnation region of a sphere or cylinder, *Int. J. Heat Mass Transfer* **23**, 179–189 (1980).
3. T. R. Fodemski and W. B. Hall, Forced convection film boiling on a sphere immersed in (a) subcooled or (b) superheated liquid, *Proc. 7th Heat Transfer Conf., Munchen* **4**, 375–379 (1982).
4. W. J. Prosnak, On the viscous flow near the stagnation point on an interface, AFOSR 1952, Princeton Univ. Dept. Aero., Eng. Rep. 563 (1961).
5. H. Schlichting, *Boundary-layer Theory*, McGraw-Hill, New York (1968).
6. B. T. Chao, Motion of spherical gas bubble in a viscous liquid at large Reynolds number, *The Physics of Fluids* **5**, 69–79 (1962).
7. D. W. Moore, The boundary layer on a spherical gas bubble, *J. Fluid Mechanics* **16**, 161–176 (1963).
8. B. T. Chao, Transient heat and mass transfer to a translating droplet, *J. Heat Transfer, Trans ASME, C*, 273–281 (1969).
9. V. K. Dhir and G. P. Purohit, Subcooled film-boiling heat transfer from spheres, *Nucl. Sci. Engng* **47**, 49–66 (1978).
10. E. Schmidt, *Properties of water and steam in SI-units*, Springer-Verlag (1969).

APPENDIX 1

Liquid velocity components and pressure gradient at the stagnation point region of an axisymmetrical particle are

$$U_x = A_1 x F_1'(\zeta_1), \tag{A1}$$

$$U_y = -\sqrt{2A_1\nu_1}\cdot F_1(\zeta), \tag{A2}$$

$$\left(-\frac{\partial p}{\partial x}\right)_1 = 2\rho_1 A_1^2 x\,[\tfrac{1}{2}F_1'^2(\zeta_1) - F_1(\zeta_1)\cdot F_1''(\zeta_1) - F_1''(\zeta_1)]. \tag{A3}$$

Assumption 3 makes possible to express function $F_1(\zeta_1)$ in the form [3, 4]

$$F_1(\zeta_1) = \zeta_1 + l(\zeta_1), \tag{A4}$$

where

$$l(\zeta_1) < \zeta_1. \tag{A5}$$

Utilizing equation (A4) in equation (1) and neglecting terms of order l^2 we have

$$l'''(\zeta_1) + \zeta_1 l''(\zeta_1) - l'(\zeta_1) = 0. \tag{A6}$$

The solution of the last equation, satisfying the condition, that far from the interface (i.e. $\zeta_1 \to \infty$) velocity is the same as in frictionless flow (i.e. $l'(\infty) \to 0$) has the form

$$l'(\zeta_1) = u_*\left[\exp(-\tfrac{1}{2}\zeta_1^2) - \sqrt{\frac{\pi}{2}}\,\zeta_1\,\mathrm{erfc}\,(\zeta_1/\sqrt{2})\right], \tag{A7}$$

where

$$u_* = l'(0) = F_1'(0) - 1. \tag{A8}$$

Integrating equation (A7) we have

$$l(\zeta_1) = \sqrt{\frac{\pi}{2}}\,u_*\left[\tfrac{1}{2}(\zeta_1^2+1)\,\mathrm{erf}\left(\frac{\zeta_1}{\sqrt{2}}\right) + \frac{\zeta_1}{\sqrt{2\pi}}\,\mathrm{e}^{-\zeta^2/2} - \frac{\zeta_1^2}{2}\right] + l(0) \tag{A9}$$

and

$$\int_0^{\zeta_1} l(\xi)\,\mathrm{d}\xi = \sqrt{\frac{\pi}{2}}\,u_*\left[\tfrac{1}{2}(\tfrac{1}{3}\zeta_1^3 + \zeta_1)\,\mathrm{erf}\left(\frac{\zeta_1}{\sqrt{2}}\right) + \frac{1}{3}\sqrt{\frac{2}{\pi}}(\tfrac{1}{2}\zeta_1^2+1)\,\mathrm{e}^{-\zeta^2/2} - \tfrac{1}{6}\zeta_1^2 - \frac{1}{3}\sqrt{\frac{2}{\pi}}\right]. \tag{A10}$$

Equations (18) and (25) using (A3), (A4), (A9), (15) and (27) can be written

$$\bar{V}_x = \tfrac{1}{2}A_1 x\{(1+u_*) + \tfrac{1}{3}\lambda_*^2[1 + u_*^2 + \sqrt{2\pi}u_* l(0) - 2u_*^2]\} \tag{A11}$$

and

$$z^2 = \lambda^2\{1 + u_*^2 + \tfrac{1}{3}\lambda_*^2[1 + u_*^2 + \sqrt{2\pi}u_*\cdot l(0)]\}. \tag{A12}$$

From (A2), (A4), (A9), (17), (20) and (A12) we have

$$l(0)=\frac{\rho_v}{\rho_l}\frac{2\kappa_v\lambda^2\{1+u_*+\frac{1}{3}\lambda_*^2[1+u_*^2+\sqrt{2\pi}u_*l(0)]\}}{\delta\sqrt{\frac{1}{2}A_l\nu_l}}. \quad (A13)$$

Finally, using equation (15), equation (A13) can be written in the form

$$l(0)=\frac{\lambda_*[1+u_*+\frac{1}{3}\lambda_*^2(1+u_*^2)]}{1-\frac{\rho_v}{\rho_l}\cdot\sqrt{\frac{\mu_v}{\mu_l}}\cdot\frac{\sqrt{2\pi}}{3}u_*\cdot\lambda_*^3}\cdot\frac{\rho_v}{\rho_l}\sqrt{\frac{\mu_v}{\mu_l}}. \quad (A14)$$

From the last equation, taking into account that $(\rho_v/\rho_l)\sqrt{(\mu_v/\mu_l)} \ll 1$ it is clear that

$$l(0) \ll 1 \cong 0, \quad (A15)$$

i.e. liquid velocity towards a particle at the interface (due to evaporation from the interface) is very small and can be neglected. Utilizing (A16) we can write

$$\begin{aligned} &F_l(\zeta_l)=\zeta_l+l(\zeta_l), && F_l(0)=l(0)\cong 0,\\ &F_l'(\zeta_l)=1+l'(\zeta_l), && F_l'(0)=1+u_*, \quad (A16)\\ &F_l''(\zeta_l)=l''(\zeta_l), && F_l''(0)=-\sqrt{\frac{\pi}{2}}u_*,\\ &F_l''(\zeta_l)=l'''(\zeta_l), && F_l'''(0)=u_*. \end{aligned}$$

Utilizing equations (A15) in equations (A1) to (A3) one can obtain liquid velocity components and the pressure gradient at the interface expressed by equations (7) to (9).

APPENDIX 2

Equation (1)—neglecting the inertia effect, i.e. terms F_vF_v'' and $F_v'^2$ simplifies to:

$$F_v'''(\zeta_v)=-\tfrac{1}{2}. \quad (A17)$$

Solution of this equation is:

$$F_v'(\zeta_v)=-\tfrac{1}{4}\zeta_v^2+C\zeta_v+C_1, \quad (A18)$$

and

$$F_v(\zeta_v)=-\tfrac{1}{12}\zeta_v^3+\tfrac{1}{2}C\zeta_l^2+C_1\zeta_v+C_2. \quad (A19)$$

Vapour velocity components are:

$$V_x=A_v(-\tfrac{1}{4}\zeta_l^2+C\zeta_v)x, \quad (A20)$$

and

$$V_y=-\sqrt{2A_v\nu_v}(-\tfrac{1}{12}\zeta_v^3+\tfrac{1}{2}C\zeta_v^2). \quad (A21)$$

In the last two equations it is assumed that $C_1 = C_2 = 0$ (at the hot surface, $\zeta_v = 0$, we have $V_x = V_y = 0$).

APPENDIX 3

Equation (33) applied to vapour gap, using equation (A19), can be written:

$$\begin{aligned} e_v(\zeta_v)&=\exp\left[-Pr_v\int_0^{\zeta_v}F_v(\xi)\,d\xi\right]\\ &=\exp\left\{-\frac{1}{6}\frac{Pr_v}{C}\zeta_v^3\left(1-\frac{\zeta_v}{8c}\right)\right\}. \quad (A22) \end{aligned}$$

Utilizing equations (14), (15) and (24) in the last expression, finally we have:

$$e_v(\zeta_l)=\exp[-g(\lambda_*,y_*)], \quad (A23)$$

and

$$e_v(\zeta_v^\delta)=\exp[-g(\lambda_*,1)]=\exp[-a(1-b)], \quad (A24)$$

where

$$g(\lambda_*,y_*)=a(\lambda_*)y_*^3[1-b(\lambda_*)y_*], \quad (A25)$$

$$a(\lambda_*)=\tfrac{2}{3}(\lambda_*\lambda_o)^2[1+u_*+\lambda_*^2(1+u_*^2)], \quad (A26)$$

and

$$b(\lambda_*)=\frac{1}{2}\frac{\lambda_*(1+u_*^2)}{1+u_*+\lambda_*^2(1+u_*^2)}. \quad (A27)$$

Now equation (34) can be written in the form:

$$E_v(\zeta_v)=\int_0^{\zeta_v}l_v(\xi)\,d\xi=\zeta_v^\delta\int_0^{y_*}\exp\{-g(\lambda_*,\xi)\}\,d\xi, \quad (A28)$$

and

$$E_v(\zeta_v^\delta)=\zeta_v^\delta\cdot\exp[-g(\lambda_*,1)]/G(\lambda_*), \quad (A29)$$

where

$$G(\lambda_*)=\left\{\exp[g(\lambda_*,1)]\int_0^1\exp[-g(\lambda_*,y_*)]\,dy_*\right\}^{-1}. \quad (A30)$$

The last coefficient must be calculated numerically.

Acknowledgements—The author wishes to acknowledge the helpful discussions he has had with Professor W. B. Hall and with members of the Safety and Reliability Directorate of the U.K. Atomic Energy Authority, and also the financial support provided by this Directorate.

INFLUENCE DE LA VISCOSITE DU LIQUIDE ET DU SYSTEME DE PRESSION SUR L'EPAISSEUR DE VAPEUR AU POINT D'ARRET PENDANT L'EBULLITION AVEC CONVECTION FORCEE

Résumé—On présente le modèle théorique de l'ébullition en convection forcée dans la région du point d'arrêt d'une particule axisymétrique. Du fait de l'effet de lubrification de l'écoulement laminaire de vapeur autour de la particule chaude, l'écoulement liquide est légèrement perturbé à partir de l'écoulement sans frottement. Cette perturbation dépend des températures de la surface de la particule, de l'écoulement libre et de saturation. Une tentative est faite pour inclure l'influence du système de pression sur le phénomène, de telle sorte que le modèle peut être utilisé pour la description de la phase de prémélange pendant l'explosion (thermique) de vapeur. L'applicabilité du modèle est montrée pour le calcul de l'épaisseur de la couche de vapeur au point d'arrêt de la sphère, et aussi des flux thermiques à l'interface et sur la surface chaude (paramètres importants qui influencent la stabilité et la disparition du film bouillant).

DER EINFLUSS DER VISKOSITÄT DER FLÜSSIGKEIT UND DES SYSTEMDRUCKES AUF DIE DICKE DES DAMPFFILMES AM STAGNATIONSPUNKT BEI FILMSIEDEN IN ERZWUNGENER STRÖMUNG

Zusammenfassung—Das Modell des Filmsiedens bei erzwungener Strömung im Bereich des Stagnationspunktes eines achsensymmetrischen Partikels wird vorgestellt. Aufgrund des 'Gleiteffekts' der laminaren Dampfströmung um das heiße Partikel weicht die Flüssigkeitsströmung nur wenig von der reibungsfreien Strömung ab. Diese Abweichung hängt von der Partikeloberfläche, der Sättigungstemperatur und von der Temperatur der ungestörten Strömung ab. Der Einfluß der Dampfgeschwindigkeit (von der Grenzfläche zur heißen Oberfläche) auf den vom Partikel abgeführten Wärmestrom wird berücksichtigt. Es wurde versucht, den Einfluß des Systemdrucks auf das Phänomen mit einzubeziehen—somit kann das vorgestellte Modell zur Beschreibung der groben Vormischphase während thermischer Dampfexplosionen eingesetzt werden. Die Anwendbarkeit des Modells zur Berechnung der Dampffilmdicke am Stagnationspunkt der Kugel und des Wärmestroms an der Grenzfläche und an der heißen Oberfläche (wichtige Parameter, die die Stabilität und das Zusammenbrechen des Filmsiedens beeinflussen) wird gezeigt.

ВЛИЯНИЕ ВЯЗКОСТИ ЖИДКОСТИ И ДАВЛЕНИЯ В СИСТЕМЕ НА ТОЛЩИНУ СЛОЯ ПАРА В ТОЧКЕ ТОРМОЖЕНИЯ ПРИ ПЛЕНОЧНОМ КИПЕНИИ В УСЛОВИЯХ ВЫНУЖДЕННОЙ КОНВЕКЦИИ

Аннотация—Предложена теоретическая модель пленочного кипения при вынужденной конвекции в области точки торможения осесимметричной частицы. Благодаря эффекту гидродинамической смазки при ламинарном обтекании нагретой частицы паром в потоке отмечается небольшое возмущение по сравнению с течением без трения. Это возмущение зависит от температур поверхности частицы и свободного потока, а также от температуры насыщения. Учитывается влияние скорости течения пара от границы раздела к нагретой поверхности на теплоперенос от частицы. Предпринята попытка учесть влияние давления в системе на исследуемый процесс и показано, что предложенная модель может быть использована для описания грубой предшествующей смешению фазы при (тепловом) взрыве пара. Показано использование модели для расчета толщины слоя пара в точке торможения сферы, а также тепловых потоков на границе раздела фаз и на нагретой поверхности, т.е. тех важных параметров, которые влияют на устойчивость и срыв пленочного кипения.